Received 13 September 2004; accepted 4 January 2005; doi:10.1038/nature03318.

1. Tabata, T. & Takei, Y. Morphogens, their identification and regulation. *Development* **131,** 703–712 (2004).
2. St Johnston, R. D. & Gelbart, W. M. *Decapentaplegic* transcripts are localized along the dorsal-ventral axis of the *Drosophila* embryo. *EMBO J.* **6,** 2785–2791 (1987).
3. Arora, K., Levine, M. S. & O'Connor, M. B. The screw gene encodes a ubiquitously expressed member of the TGF-β family required for specification of dorsal cell fates in the *Drosophila* embryo. *Genes Dev.* **8,** 2588–2601 (1994).
4. Dorfman, R. & Shilo, B. Z. Biphasic activation of the BMP pathway patterns the *Drosophila* embryonic dorsal region. *Development* **128,** 965–972 (2001).
5. Irish, V. F. & Gelbart, W. M. The *decapentaplegic* gene is required for dorsal-ventral patterning of the *Drosophila* embryo. *Genes Dev.* **1,** 868–879 (1987).
6. Rushlow, C., Colosimo, P. F., Lin, M. C., Xu, M. & Kirov, N. Transcriptional regulation of the *Drosophila* gene *zen* by competing Smad and Brinker inputs. *Genes Dev.* **15,** 340–351 (2001).
7. Ross, J. J. *et al.* Twisted gastrulation is a conserved extracellular BMP antagonist. *Nature* **410,** 479–483 (2001).
8. Ferguson, E. L. & Anderson, K. V. Decapentaplegic acts as a morphogen to organize dorsal-ventral pattern in the *Drosophila* embryo. *Cell* **71,** 451–461 (1992).
9. Brummel, T. J. *et al.* Characterization and relationship of Dpp receptors encoded by the *saxophone* and *thick veins* genes in *Drosophila*. *Cell* **78,** 251–261 (1994).
10. Penton, A. *et al.* Identification of two bone morphogenetic protein type I receptors in *Drosophila* and evidence that Brk25D is a *decapentaplegic* receptor. *Cell* **78,** 239–250 (1994).
11. Letsou, A. *et al.* *Drosophila* Dpp signaling is mediated by the *punt* gene product: a dual ligand-binding type II receptor of the TGF-β receptor family. *Cell* **80,** 899–908 (1995).
12. Teleman, A. A. & Cohen, S. M. Dpp gradient formation in the *Drosophila* wing imaginal disc. *Cell* **103,** 971–980 (2000).
13. Kosman, D. & Small, S. Concentration-dependent patterning by an ectopic expression domain of the *Drosophila* gap gene *knirps*. *Development* **124,** 1343–1354 (1997).
14. Decotto, E. & Ferguson, E. L. A positive role for Short gastrulation in modulating BMP signaling during dorsoventral patterning in the *Drosophila* embryo. *Development* **128,** 3831–3841 (2001).
15. Eldar, A. *et al.* Robustness of the BMP morphogen gradient in *Drosophila* embryonic patterning. *Nature* **419,** 304–308 (2002).
16. Shimmi, O. & O'Connor, M. B. Physical properties of Tld, Sog, Tsg and Dpp protein interactions are predicted to help create a sharp boundary in Bmp signals during dorsoventral patterning of the *Drosophila* embryo. *Development* **130,** 4673–4682 (2003).
17. Holley, S. A. *et al.* The *Xenopus* dorsalizing factor Noggin ventralizes *Drosophila* embryos by preventing DPP from activating its receptor. *Cell* **86,** 607–617 (1996).
18. Ashe, H. L. & Levine, M. Local inhibition and long-range enhancement of Dpp signal transduction by Sog. *Nature* **398,** 427–431 (1999).
19. Marques, G. *et al.* Production of a DPP activity gradient in the early *Drosophila* embryo through the opposing actions of the SOG and TLD proteins. *Cell* **91,** 417–426 (1997).
20. Oelgeschlager, M. *et al.* The pro-BMP activity of Twisted gastrulation is independent of BMP binding. *Development* **130,** 4047–4056 (2003).
21. Neul, J. L. & Ferguson, E. L. Spatially restricted activation of the SAX receptor by SCW modulates DPP/TKV signaling in *Drosophila* dorsal-ventral patterning. *Cell* **95,** 483–494 (1998).
22. Nguyen, M., Park, S., Marques, G. & Arora, K. Interpretation of a BMP activity gradient in *Drosophila* embryos depends on synergistic signaling by two type I receptors, SAX and TKV. *Cell* **95,** 495–506 (1998).
23. Shimmi, O., Umulis, D., Othmer, H. & O'Connor, M. B. Facilitated transport of a Dpp/Scw heterodimer by Sog/Tsg leads to robust patterning of the *Drosophila* blastoderm embryo. *Cell* (in the press).
24. Mason, E. D., Williams, S., Grotendorst, G. R. & Marsh, J. L. Combinatorial signaling by Twisted Gastrulation and Decapentaplegic. *Mech. Dev.* **64,** 61–75 (1997).
25. Wisotzkey, R. G. *et al.* *Medea* is a *Drosophila Smad4* homolog that is differentially required to potentiate DPP responses. *Development* **125,** 1433–1445 (1998).
26. Rushlow, C., Doyle, H., Hoey, T. & Levine, M. Molecular characterization of the *zerknullt* region of the *Antennapedia* gene complex in *Drosophila*. *Genes Dev.* **1,** 1268–1279 (1987).
27. Ferrell, J. E. Self-perpetuating states in signal transduction: positive feedback, double-negative feedback and bistability. *Curr. Opin. Cell Biol.* **14,** 140–148 (2002).
28. Lai, K., Robertson, M. J. & Schaffer, D. V. The Sonic hedgehog signaling system as a bistable genetic switch. *Biophys. J.* **86,** 2748–2757 (2004).
29. Stein, D., Roth, S., Vogelsang, E. & Nusslein-Volhard, C. The polarity of the dorsoventral axis in the *Drosophila* embryo is defined by an extracellular signal. *Cell* **65,** 725–735 (1991).
30. Little, S. C. & Mullins, M. C. Twisted gastrulation promotes BMP signaling in zebrafish dorsal-ventral axial patterning. *Development* **131,** 5825–5835 (2004).
31. Xie, J. & Fisher, S. Twisted gastrulation enhances BMP signaling through chordin dependent and independent mechanisms. *Development* **132,** 383–391 (2005).

Supplementary Information accompanies the paper on **www.nature.com/nature**.

Acknowledgements We thank N. Dostatni, M. Levine and M. Markstein for fly stocks; S. Cohen, M. Levine and M. Markstein for plasmids; P. ten Dijke and C. Heldin for antibodies; V. Bindokas for assistance with confocal microscopy; S. Lemke and M. Markstein for discussions; D. Bishop, M. O. Casanueva, C. Li, A. Mahowald, J. Malamy, M. Markstein, V. Prince and J. Staley for helpful comments on the manuscript, and M. O'Connor for sharing unpublished data and reagents. Preliminary data on the second function of Tsg were obtained by E. Decotto. Funding was provided by grants to E.L.F. from the NIH and from the Human Frontiers Science program.

Competing interests statement The authors declare that they have no competing financial interests.

Correspondence and requests for materials should be addressed E.L.F. (elfergus@midway.uchicago.edu).

The immunoglobulin superfamily protein Izumo is required for sperm to fuse with eggs

Naokazu Inoue[1], Masahito Ikawa[2], Ayako Isotani[1,3] & Masaru Okabe[1,2,3]

[1]*Genome Information Research Center,* [2]*Research Institute for Microbial Diseases,* [3]*Faculty of Pharmaceutical Sciences, Osaka University, Yamadaoka 3-1, Suita, Osaka 565-0871, Japan*

Representing the 60 trillion cells that build a human body, a sperm and an egg meet, recognize each other, and fuse to form a new generation of life. The factors involved in this important membrane fusion event, fertilization, have been sought for a long time[1]. Recently, CD9 on the egg membrane was found to be essential for fusion[2–4], but sperm-related fusion factors remain unknown. Here, by using a fusion-inhibiting monoclonal antibody[5] and gene cloning, we identify a mouse sperm fusion-related antigen and show that the antigen is a novel immunoglobulin superfamily protein. We have termed the gene *Izumo* and produced a gene-disrupted mouse line. *Izumo*$^{-/-}$ mice were healthy but males were sterile. They produced normal-looking sperm that bound to and penetrated the zona pellucida but were incapable of fusing with eggs. Human sperm also contain Izumo and addition of the antibody against human Izumo left the sperm unable to fuse with zona-free hamster eggs.

To identify factors involved in sperm–egg fusion, we used a monoclonal antibody, OBF13, against mouse sperm that specifically inhibits the fusion process[5]. The antigen was identified by separation of the crude extracts from mouse sperm by two-dimensional gel electrophoresis and subsequent immunoblotting with the monoclonal antibody. We termed the antigen 'Izumo' after a Japanese shrine dedicated to marriage. The identified spot was analysed by liquid chromatography tandem mass spectrometry (LC–MS/MS), and ten peptides that were 100% identical to a part of the sequence listed in the RIKEN full-length database (National Centre for Biotechnology Information (NCBI) accession number XM_133424) were found. The registered DNA sequence was confirmed by sequencing after polymerase chain reaction with reverse transcription (RT–PCR) with total RNA prepared from the testis. A human homologue was found as an unverified gene in the NCBI database (accession number BC034769). The gene encodes a novel immunoglobulin superfamily (IgSF), type I membrane protein with an extracellular immunoglobulin domain that contains one putative glycosylation site (Fig. 1a, b). Mouse Izumo was shown to be a testis (sperm)-specific 56.4-kDa antigen by western blotting with a polyclonal antibody raised against recombinant mouse Izumo (Fig. 1c). Izumo was also detectable as a 37.2-kDa protein by western blotting of human sperm with anti-human Izumo antibody (Fig. 1d). Izumo was not detectable on the surface of fresh sperm. Coinciding with the fact that mammalian sperm are incapable of fertilizing eggs when ejaculated and that fertilization occurs only after an exocytotic process called the acrosome reaction, both mouse and human Izumo became detectable on sperm surface only after the acrosome reaction (Fig. 1e, f). This would probably be because Izumo is not localized on plasma membrane of fresh spermatozoa but is hidden under plasma membrane and accessible after the acrosome reaction, as occurs with CD46 on mouse sperm[6].

To address the physiological role of Izumo *in vivo* we generated *Izumo*-deficient mice by homologous recombination. An *Izumo*-targeting construct was designed to replace exons 2–10 with a neomycin-resistant gene (*neo*^{r}) (Fig. 2a). Both the targeting event in D3 embryonic stem cells and the germline transmission of targeted genes were confirmed by Southern blot analysis (Fig. 2b).

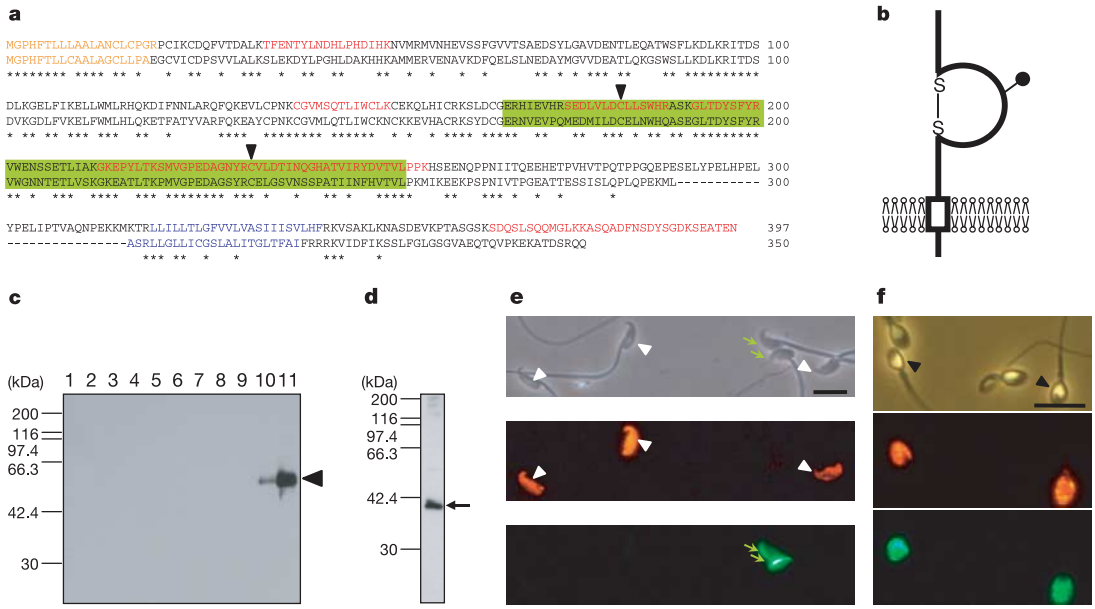

Figure 1 Identification and characterization of *Izumo*. **a**, Amino-acid sequences of mouse (upper) and human (lower) Izumo. Amino-acid identity is indicated by an asterisk. The peptide sequences obtained by LC–MS/MS are shown in red. The putative signal peptide and transmembrane region are shown in orange and blue, respectively. The immunoglobulin-like domain is boxed in green. The cysteine residues that might form a disulphide bridge are indicated by arrowheads. **b**, Izumo is a typical type I membrane glycoprotein with one immunoglobulin-like domain and a putative *N*-glycoside link motif (Asn 204). **c**, Izumo was detected exclusively in testis and sperm by western blotting. The tissues examined are, from left to right: brain, heart, thymus, spleen, lung, liver, muscle, kidney, ovary, testis and sperm. All solubilized proteins were loaded at 30 μg on each lane and detected by 1 μg ml^{-1} anti-mouse Izumo antibody. The arrowhead indicates mouse Izumo protein. **d**, Western blotting analysis of human Izumo protein from human sperm. The arrow indicates human Izumo protein. **e**, Immunostaining of Izumo in sperm from an acrosin-promoter-driven transgenic mouse line that has enhanced green fluorescent protein in the acrosome. Izumo was not detected in fresh sperm with intact acrosomes expressing EGFP[30] (indicated by green arrows), but was revealed on acrosome-reacted (non-green fluorescent) sperm (stained red, shown by white arrowheads), when stained with the polyclonal antibody against mouse Izumo. **f**, Human sperm were also stained with polyclonal anti-human Izumo antibody (red). Acrosome-reacted human sperm (stained green with anti-CD46 antibody[31]) were reactive to the antibody against human Izumo but the same antibody did not react to acrosome-intact (CD46-negative) sperm. Scale bar, 10 μm.

In the homozygous mutant mice, the full-length (1.6-kilobase (kb)) messenger RNA (Fig. 2c) and the Izumo protein (Fig. 2d) were not detected. Because the disruption of a gene can cause a concomitant increase or decrease in some related genes[7], we examined ADAM2 (ref. 8), CD147 (ref. 9) and sp56 (ref. 10), which were reported to be involved in sperm–egg interactions. We could not find a significant change in these protein levels in sperm after the deletion of *Izumo* gene (Fig. 2d).

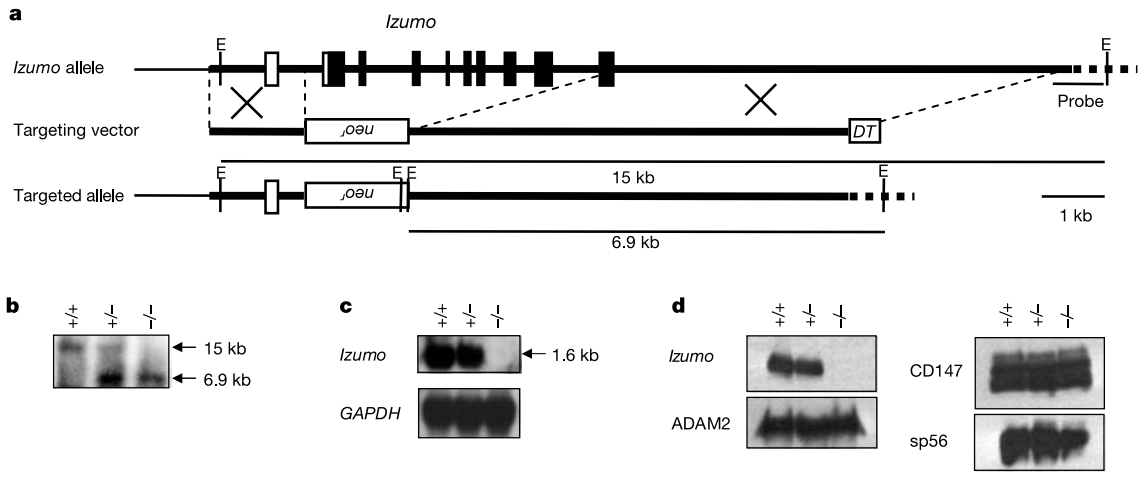

Figure 2 Targeted disruption of *Izumo* gene. **a**, Complete structures of the wild-type mouse *Izumo* allele, targeting vector and mutant allele. Exons and introns are represented by vertical bars and horizontal lines, respectively. A neomycin-resistance gene driven by a phosphoglycerine kinase (PGK) promoter (*neo*^{r}) and a diphtheria toxin A chain driven by a MC1 promoter (DT) are shown as white boxes. **b**, Southern blot genotyping confirmed gene disruption. Hybridization of the 3′ external probe with *Eco*RI-digested genomic DNA yielded 15-kb (wild type) and 6.9-kb (mutant) bands. **c**, Northern blot of total testis RNA (20 μg) from wild-type (+/+), heterozygous (+/−) and homozygous (−/−) mice. GAPDH is shown as a loading control. **d**, By western blotting, Izumo protein was undetectable in mutant mice. Various sperm proteins (30 μg per lane) were detectable by western blotting in sperm from *Izumo*$^{-/-}$ mice as well as wild-type and heterozygous animals. From the top, Izumo, ADAM2 (9D2.2; Chemicon), CD147 (Santa Cruz) and sp56 (7C5; QED Biologicals) are shown.

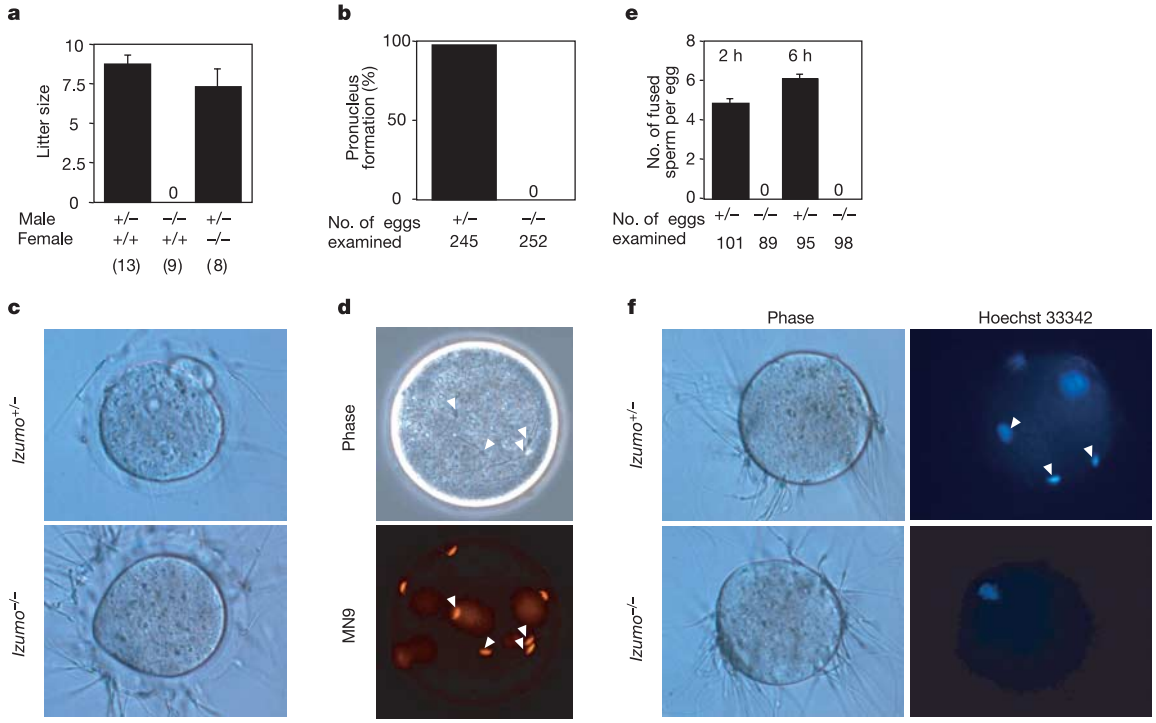

Figure 3 Male infertility caused by *Izumo* disruption. **a**, Fecundity of *Izumo*$^{+/-}$ and *Izumo*$^{-/-}$ males and *Izumo*$^{-/-}$ females. The numbers in parentheses indicate the numbers of mating pairs. **b**, **c**, *In vitro* fertilization of sperm from *Izumo*$^{+/-}$ and *Izumo*$^{-/-}$ mice. Unlike *Izumo*$^{+/-}$, the eggs inseminated with *Izumo*$^{-/-}$ sperm had many sperm on their zona pellucida, owing to the failure of sperm–egg fusion that probably leads to the absence of zona-reaction to lessen the sperm-binding ability of the zona pellucida. The error bars in **b** are not visible ($n = 5$). **d**, Upper panel, accumulation of many sperm in the perivitelline space of the eggs recovered from the females mated with *Izumo*$^{-/-}$ males. Lower panel, sperm in perivitelline space labelled with acrosome-reacted, sperm-specific monoclonal antibody MN9 (ref. 15). **e**, Average numbers of fused sperm observed 2 and 6 h after insemination ($n = 5$). **f**, Fused sperm stained by Hoechst 33342 preloaded into the egg. The arrowheads show the fused sperm. Errors bars in **a** and **e** are s.e.m.

Intercrosses between heterozygous F_1 mice yielded offspring that segregated in a mendelian distribution: 43 wild-type, 92 heterozygous and 47 homozygous mutant weaning pups. *Izumo*$^{-/-}$ mutant mice were healthy and showed no overt developmental abnormalities. *Izumo*$^{-/-}$ females demonstrated normal fecundity. *Izumo*$^{+/-}$ males also showed normal fertilizing ability (Fig. 3a). However, *Izumo*$^{-/-}$ males were sterile despite normal mating behaviour and ejaculation, with normal vaginal plug formations. After observation of 28 plugs, nine pairs of *Izumo*$^{-/-}$ male and wild-type females were kept for another 4 months but no pregnancies were observed (Fig. 3a). In at least four different cases of gene knockouts that resulted in male sterility attributed to impaired zona-binding ability, the sperm also failed to migrate into the oviduct[7,8,11,12]. However, disruption of *Izumo* did not cause any defect in sperm migration into the oviduct (data not shown, and there was no reduction of sperm motility in *Izumo*$^{-/-}$ sperm; motility was measured 120 min after incubation by computer-aided sperm analysis (CASA; mean ± s.e.m. = 81.7 ± 7.7% in *Izumo*$^{+/-}$ sperm and 77 ± 8.9% in *Izumo*$^{-/-}$ sperm)). The sterile nature of *Izumo*$^{-/-}$ sperm was shown in the *in vitro* fertilization system (Fig. 3b, c, and Supplementary Movie 1). The impaired fertilization step undoubtedly followed zona penetration because sperm penetrated the zona pellucida and accumulated in the perivitelline space of the eggs (Fig. 3d).

Syngamy can be considered to occur to two stages: binding of the sperm plasma membrane to that of the egg, and actual membrane fusion. *Izumo*$^{-/-}$ sperm were capable of binding to the plasma membranes of eggs whose zona pellucida had been mechanically removed[13](Fig. 3e, f). In this system, the *Izumo*$^{+/-}$ sperm incubated for 2 and 6 h fused to eggs in approximate ratios of 4.5 and 6 sperm per egg, respectively, but no *Izumo*$^{-/-}$ sperm fused with eggs.

Sperm cannot fuse with eggs unless the former have undergone the acrosome reaction[14]. To verify the acrosomal status of *Izumo*$^{-/-}$ sperm, we stained the sperm accumulated in perivitelline spaces with the MN9 monoclonal antibody, which immunoreacts only to the equatorial segment of acrosome-reacted sperm[15]. The staining indicated that the *Izumo*$^{-/-}$ sperm had undergone the acrosome reaction (Fig. 3d) but failed to fuse with eggs.

Because no offspring were fathered by *Izumo*$^{-/-}$ male mice, it was unclear whether the defect was limited to fusion or extended to later developmental stages. To address this question, we used intracytoplasmic sperm injection (ICSI) to insert *Izumo*$^{-/-}$ sperm directly into the cytoplasm of wild-type eggs and bypass the fusion step[16]. Eggs injected with *Izumo*$^{-/-}$ sperm were successfully activated and the fertilized eggs were transplanted into the oviducts of pseudopregnant females. The eggs implanted normally and the resulting embryos developed appropriately to term with rates similar to those of heterozygous mice (Table 1).

Sperm–egg fusion is known to be less species-specific than sperm–zona interaction. For example, human sperm cannot penetrate the hamster zona pellucida but they can fuse with zona-free hamster eggs, and this system (zona-free hamster-egg sperm

Table 1 **Development of eggs after ICSI with *Izumo*$^{-/-}$ sperm**

Sperm	No. of eggs used	No. of eggs surviving after ICSI	No. of eggs developing to two-cell stage	No. of pups born
Izumo$^{-/-}$	95	59	42 (71%)*	12 (29%)†
Izumo$^{+/-}$	85	54	43 (80%)	6 (14%)

*Percentages are based on numbers of eggs surviving after ICSI.
†All offspring from *Izumo*$^{-/-}$ sperm were confirmed to possess the *Izumo*-null allele.

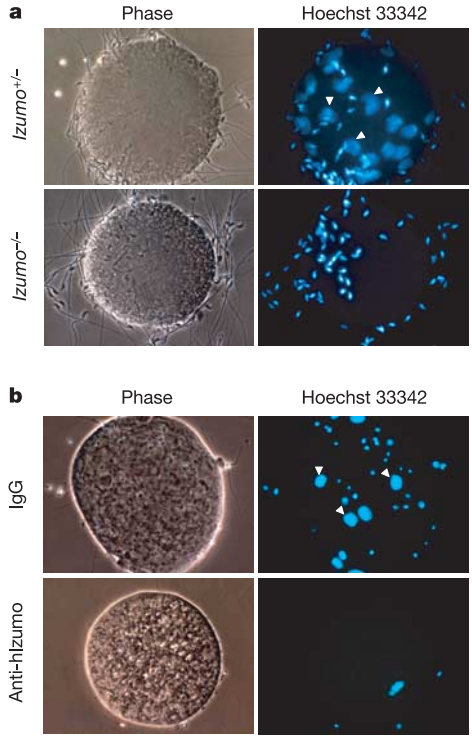

Figure 4 Involvement of Izumo in a xeno-species fusion system. **a**, At 6 h after the insemination of zona-free hamster eggs with *Izumo* $^{+/-}$ and *Izumo* $^{-/-}$ mouse sperm, sperm heads were stained by adding Hoechst 33342 to the medium. The sperm–egg binding was strong enough to resist repeated pipetting. **b**, Human sperm were also added with 25 μg ml^{-1} anti-human Izumo (anti-hIzumo) or control IgG to zona-free hamster eggs (n=3). No fusion was observed in the presence of anti-Izumo antibody. Arrowheads indicate the swelling sperm head after staining with Hoechst 33342. The eggs were pressed under a coverslip to bring many sperm into focus.

penetration test) has been used for the assessment of human sperm fertility[17]. We first examined the contribution of mouse Izumo in a zona-free hamster-egg sperm penetration assay. As indicated in Fig. 4a, the mouse Izumo was essential not only in the homologous fusion system but also for heterologous fusion with hamster eggs. Similarly, when the anti-human Izumo polyclonal antibody was added to the incubation mixture, no fusion was observed, whereas the sperm treated with control IgG fused with eggs at an average of 5.9 ± 0.7 sperm per egg. The total numbers of eggs observed were 23 and 29, respectively (n=3). These results indicated that human Izumo is involved in the fertilization process in human sperm (Fig. 4b). However, further investigation will be required to explain the function of Izumo in human fertilization because adding the antibody caused inhibition of human sperm binding to the egg plasma membrane in the heterologous sperm–egg fusion system.

The phenotypes of gene knockout mice are not always related to the disrupted genes but are sometimes caused by disruption of a neighbouring gene[18]. To examine whether the phenotype was directly derived from the lack of Izumo on sperm, we performed a rescue experiment by crossing *Izumo* $^{-/-}$ mice with transgenic mouse lines generated to express Izumo by using the testis-specific calmegin promoter[12]. The sterile phenotype was rescued with the transgenically expressed Izumo on mouse sperm (Supplementary Fig. 1).

In the search for sperm surface proteins that function in sperm–egg plasma-membrane binding and fusion, various candidates such as DE[19], CD46 (ref. 20), equatorin[15], Sperad[21] and SAMP32 (ref. 22) have been reported. ADAM family proteins are given the most attention for their possession of a putative fusion peptide (ADAM1) and disintegrin domain (ADAM2 and ADAM3)[23]. None of the mice possessing disrupted ADAM1a, ADAM2 and ADAM3 show a significant defect in the ability to fuse with eggs[7,8,24], but do show an impairment of sperm–zona binding ability. Similarly, CD46 disruption does not diminish fusion[6]. In contrast, CD9 on the egg surface is essential for the fusing ability of eggs[2–4] and some indications for the involvement of the binding of integrins to CD9 are postulated in reference to sperm–egg fusion. However, the disruptions of the most probable candidate integrins α6 and β1 cause no major influence on the fusing ability of eggs[25]. Thus, for several years, postulated fertilization mechanisms were repeatedly changed as a result of gene disruption experiments. This suggests that the essential nature of the candidate gene must be judged after observing the phenotype of the gene-disrupted mice. In this context, Izumo is the first sperm membrane protein shown to be essential for fusion. It is not yet known whether sperm Izumo interacts with egg CD9, as occurs with placental IgSF protein PSG17 (ref. 26); neither do we know why the localization of Izumo after acrosome reaction is not limited to the equatorial segment where fusion initially takes place. All we can say now is that continued study of this protein's function will undoubtedly lead to a fuller understanding of the cell–cell fusion process in fertilization and perhaps in other somatic systems such as muscle cells or trophoblasts.

The finding not only provides insight into the enigmatic fusion mechanism but also promises benefits in the clinical treatment of infertility and the potential development of new contraceptive strategies. □

Methods

Cloning of *Izumo*

Izumo amino acid sequences were determined by combining two-dimensional gel electrophoresis and LC–MS/MS. Some peptide sequences (Fig. 1a, shown in red) were analysed and identified as members of an immunoglobulin superfamily protein (NCBI accession number XM_133424) whose function was not clarified. To confirm the DNA sequence we used RT–PCR to amplify Izumo from mouse testis RNA as a template with primers derived from this sequence. The polyclonal antibodies against mouse and human Izumo were produced by immunizing an Izumo-expressing RK13 cell line into rabbits[27].

Generation of *Izumo* knockout mice

A targeting vector was constructed with the use of pMulti-ND 1.0 containing the Neo-resistance gene (*neo*^{r}) as a positive selection marker and diphtheria toxin A chain (DT) as a negative selection marker (provided by J. Takeda and T. Ijiri). A 1.7-kb *Asc*I–*Pac*I fragment and a 6.7-kb *Cla*I–*Xho*I fragment were inserted as a short and long arm, respectively. Embryonic stem cells derived from 129/Sv (D3) were electroporated with *Pme*I-digested linearized DNA. Of 385 G418-resistant clones, four had undergone homologous recombination correctly. Three targeted cell lines were injected into C57BL/6 blastocysts, resulting in the birth of male chimaeric mice. These mice were then crossed with C57BL/6 to obtain heterozygous mutants. Mice used in the study were the offspring of crosses between F_1 and/or F_2 generations.

In vitro fertilization

Mouse sperm were collected from cauda epididymides and capacitated *in vitro* for 2 h in a 200-μl drop of TYH medium[28] covered with paraffin oil. Wild-type female mice (more than 8 weeks old) were superovulated by the injection of 5 U of human chorionic gonadotropin (hCG) 48 h after a 5-U injection of pregnant mare serum gonadotropin. The eggs were collected from the oviduct 14 h after the hCG injection. Eggs were placed in a 200-μl drop of TYH medium. These eggs were incubated with 2×10^5 *Izumo* $^{+/-}$ or *Izumo* $^{-/-}$ sperm per ml incubated for 2 h at 37 °C in 5% CO_2, and unbound sperm were washed away. Eggs were observed 6 h after insemination for the formation of pronuclei under a Hoffman modulation contrast microscope.

Zona-free-egg sperm penetration assay

After being freed from cumulus cells with 0.01% (w/v) hyaluronidase, the zona pellucida was removed from mouse or hamster eggs with a piezo-manipulator as described previously[13]. Fusion assessment was performed in two different ways. In the first method, zona-free mouse oocytes were preloaded with Hoechst 33342 by incubating them with the dye (1 μg ml^{-1}) in TYH for 10 min and washing them before addition of the sperm. After 30 min of incubation, the eggs were observed under a fluorescence microscope (excitation with ultraviolet) after fixing with 0.25% glutaraldehyde. This procedure enabled the staining of only fused sperm nuclei by transferring the dye into sperm after membrane fusion as in Fig. 3. Alternatively, in the second method the zona-free hamster eggs were incubated for 6 h with sperm without preloading of the dye. By this time, enlarged sperm heads could be seen when fusion occurred. The eggs with sperm were incubated in 1 μg ml^{-1} Hoechst 33342 for 10 min to ensure that all bound (original sperm head shape) and fused (enlarged round shape) sperm would be stained with the dye, as in Fig. 4. In all

experiments the human sperm were collected from liquefied semen by the swim-up method and incubated for 6 h before addition to eggs. We used BWW medium[29] containing 35 mg ml^{-1} human serum albumin (HSA) for the human sperm experiment.

Received 12 October 2004; accepted 17 January 2005; doi:10.1038/nature03362.

1. Stein, K. K., Primakoff, P. & Myles, D. Sperm–egg fusion: events at the plasma membrane. *J. Cell Sci.* **117,** 6269–6274 (2004).
2. Miyado, K. *et al.* Requirement of CD9 on the egg plasma membrane for fertilization. *Science* **287,** 321–324 (2000).
3. Le Naour, F., Rubinstein, E., Jasmin, C., Prenant, M. & Boucheix, C. Severely reduced female fertility in CD9-deficient mice. *Science* **287,** 319–321 (2000).
4. Kaji, K. *et al.* The gamete fusion process is defective in eggs of CD9-deficient mice. *Nature Genet.* **24,** 279–282 (2000).
5. Okabe, M. *et al.* Capacitation-related changes in antigen distribution on mouse sperm heads and its relation to fertilization rate *in vitro*. *J. Reprod. Immunol.* **11,** 91–100 (1987).
6. Inoue, N. *et al.* Disruption of mouse CD46 causes an accelerated spontaneous acrosome reaction in sperm. *Mol. Cell. Biol.* **23,** 2614–2622 (2003).
7. Nishimura, H., Kim, E., Nakanishi, T. & Baba, T. Possible function of the ADAM1a/ADAM2 fertilin complex in the appearance of ADAM3 on the sperm surface. *J. Biol. Chem.* **279,** 34957–34962 (2004).
8. Cho, C. *et al.* Fertilization defects in sperm from mice lacking fertilin beta. *Science* **281,** 1857–1859 (1998).
9. Saxena, D. K., Oh-Oka, T., Kadomatsu, K., Muramatsu, T. & Toshimori, K. Behaviour of a sperm surface transmembrane glycoprotein basigin during epididymal maturation and its role in fertilization in mice. *Reproduction* **123,** 435–444 (2002).
10. Bookbinder, L. H., Cheng, A. & Bleil, J. D. Tissue- and species-specific expression of sp56, a mouse sperm fertilization protein. *Science* **269,** 86–89 (1995).
11. Hagaman, J. R. *et al.* Angiotensin-converting enzyme and male fertility. *Proc. Natl Acad. Sci. USA* **95,** 2552–2557 (1998).
12. Ikawa, M. *et al.* Calmegin is required for fertilin alpha/beta heterodimerization and sperm fertility. *Dev. Biol.* **240,** 254–261 (2001).
13. Yamagata, K. *et al.* Sperm from the calmegin-deficient mouse have normal abilities for binding and fusion to the egg plasma membrane. *Dev. Biol.* **250,** 348–357 (2002).
14. Yanagimachi, R. *Mammalian Fertilization* (eds Knobil, E & Neill, J. D.) (Raven, New York, 1994).
15. Manandhar, G. & Toshimori, K. Exposure of sperm head equatorin after acrosome reaction and its fate after fertilization in mice. *Biol. Reprod.* **65,** 1425–1436 (2001).
16. Kimura, Y. & Yanagimachi, R. Intracytoplasmic sperm injection in the mouse. *Biol. Reprod.* **52,** 709–720 (1995).
17. Yanagimachi, R., Yanagimachi, H. & Rogers, B. J. The use of zona-free animal ova as a test-system for the assessment of the fertilizing capacity of human spermatozoa. *Biol. Reprod.* **15,** 471–476 (1976).
18. Olson, E. N., Arnold, H. H., Rigby, P. W. & Wold, B. J. Know your neighbors: three phenotypes in null mutants of the myogenic bHLH gene MRF4. *Cell* **85,** 1–4 (1996).
19. Rochwerger, L., Cohen, D. J. & Cuasnicu, P. S. Mammalian sperm–egg fusion: the rat egg has complementary sites for a sperm protein that mediates gamete fusion. *Dev. Biol.* **153,** 83–90 (1992).
20. Anderson, D. J., Abbott, A. F. & Jack, R. M. The role of complement component C3b and its receptors in sperm–oocyte interaction. *Proc. Natl Acad. Sci. USA* **90,** 10051–10055 (1993).
21. Ilayperuma, I. Identification of the 48-kDa G11 protein from guinea pig testes as sperad. *J. Exp. Zool.* **293,** 617–623 (2002).
22. Hao, Z. *et al.* SAMP32, a testis-specific, isoantigenic sperm acrosomal membrane-associated protein. *Biol. Reprod.* **66,** 735–744 (2002).
23. Blobel, C. P. *et al.* A potential fusion peptide and an integrin ligand domain in a protein active in sperm–egg fusion. *Nature* **356,** 248–252 (1992).
24. Nishimura, H., Cho, C., Branciforte, D. R., Myles, D. G. & Primakoff, P. Analysis of loss of adhesive function in sperm lacking cyritestin or fertilin beta. *Dev. Biol.* **233,** 204–213 (2001).
25. He, Z. Y. *et al.* None of the integrins known to be present on the mouse egg or to be ADAM receptors are essential for sperm–egg binding and fusion. *Dev. Biol.* **254,** 226–237 (2003).
26. Ellerman, D. A., Ha, C., Primakoff, P., Myles, D. G. & Dveksler, G. S. Direct binding of the ligand PSG17 to CD9 requires a CD9 site essential for sperm–egg fusion. *Mol. Biol. Cell* **14,** 5098–5103 (2003).
27. Inoue, N. *et al.* A novel chicken membrane-associated complement regulatory protein: molecular cloning and functional characterization. *J. Immunol.* **166,** 424–431 (2001).
28. Toyoda, Y., Yokoyama, M. & Hoshi, T. Studies on the fertilization of mouse egg *in vitro*. *Jpn. J. Anim. Reprod.* **16,** 147–151 (1971).
29. Overstreet, J. W., Yanagimachi, R., Katz, D. F., Hayashi, K. & Hanson, F. W. Penetration of human spermatozoa into the human zona pellucida and the zona-free hamster egg: a study of fertile donors and infertile patients. *Fertil. Steril.* **33,** 534–542 (1980).
30. Nakanishi, T. *et al.* Real-time observation of acrosomal dispersal from mouse sperm using GFP as a marker protein. *FEBS Lett.* **449,** 277–283 (1999).
31. Okabe, M. *et al.* A human sperm antigen possibly involved in binding and/or fusion with zona-free hamster eggs. *Fertil. Steril.* **54,** 1121–1126 (1990).

Supplementary Information accompanies the paper on **www.nature.com/nature**.

Acknowledgements We thank K. Toshimori for providing anti-MN9 antibody; K. Yamagata for discussions; G. L. Gerton and S. Moss for critically reviewing the draft; and Y. Maruyama, A. Kawai and Y. Koreeda for technical assistance with gene disruption. This work was supported by grant-in-aid for Scientific Research and the 21st Century COE program from the Ministry of Education, Culture, Sports, Science, and Technology of Japan.

Competing interests statement The authors declare that they have no competing financial interests.

Correspondence and requests for materials should be addressed to M.O. (e-mail: okabe@gen-info.osaka-u.ac.jp). Sequences have been deposited with GenBank under accession numbers AB195681 for mouse *Izumo*, AB195682 for human *Izumo* and AB195683 for rat *Izumo*.

Agonist/endogenous peptide–MHC heterodimers drive T cell activation and sensitivity

Michelle Krogsgaard[1], Qi-jing Li[1], Cenk Sumen[1]*, Johannes B. Huppa[1,2], Morgan Huse[1] & Mark M. Davis[1,2]

[1]*The Department of Microbiology and Immunology, and* [2]*Howard Hughes Medical Institute, Stanford University School of Medicine, Stanford, California 94305, USA*

* Present address: Center for Blood Research, Harvard Medical School, Boston, Massachusetts 02115, USA

αβ T lymphocytes are able to detect even a single peptide–major histocompatibility complex (MHC) on the surface of an antigen-presenting cell[1,2]. This is despite clear evidence, at least with CD4$^+$ T cells, that monomeric ligands are not stimulatory[3,4]. In an effort to understand how this remarkable sensitivity is achieved, we constructed soluble peptide–MHC heterodimers in which one peptide is an agonist and the other is one of the large number of endogenous peptide–MHCs displayed by presenting cells. We found that some specific combinations of these heterodimers can stimulate specific T cells in a CD4-dependent manner. This activation is severely impaired if the CD4-binding site on the agonist ligand is ablated, but the same mutation on an endogenous ligand has no effect. These data correlate well with analyses of lipid bilayers and cells presenting these ligands, and indicate that the basic unit of helper T cell activation is a heterodimer of agonist peptide– and endogenous peptide–MHC complexes, stabilized by CD4.

It has been known for some time that αβ T-cell antigen receptor (TCR)-bearing T cells are selected for weak or rare interactions with some of the thousands of self-peptide–MHC (pMHC) complexes (that is, endogenous peptide–MHC complexes) presented in the thymus and also require the presence of these complexes in the periphery to survive[5–7]. However, the role of self-peptide–MHC complexes in the activation of mature T cells is controversial. Although there is some evidence to suggest that endogenous peptides or their mimics enhance CD4$^+$ helper T cell activation[8], and that T cell responsiveness declines rapidly in the absence of endogenous pMHC contact[7], others working with CD8$^+$ T cells have found no effect[9]. Recently, we have found that there is a substantial (~20%) recruitment of endogenous peptide–MHC molecules into the immunological synapse[1,8]. This seems to be driven by weak interactions with TCRs. This phenomenon, together with data showing that even a single agonist peptide–MHC complex can initiate T cell activation[1,2] has led to the suggestion of a 'pseudodimer' model of T cell activation, in which agonist and endogenous peptide–MHC complexes, stabilized by CD4, are crucial intermediates for triggering CD4$^+$ T lymphocytes[1].

To test this model, we used the well-characterized moth cytochrome *c* (MCC) system in which specific T cells bearing the 5C.C7 TCR recognize MCC bound to the murine MHC class II molecule I-E^k (ref. 10). We looked at the T cell–antigen-presenting cell (APC) synapse and measured the accumulation of MCC and its variants as well as a spectrum of self-peptide ligands previously found to be associated with I-E^k (refs 8, 11, 12; Fig. 1a). In these assays, we used *in vitro*-stimulated lymph node cells isolated from 5C.C7-αβ TCR transgenic mice[10]. These T cell blasts were mixed with APCs that had been loaded with a strong agonist variant of MCC (K5), and the peptide being analysed was labelled with Cy3. The mixture was imaged by time-lapse three-dimensional (3D) fluorescence microscopy. Figure 1b shows representative images of pMHC accumulation at the T cell–APC interface. Consistent with previous